UNIVERSITY OF
LINCOLN

Research Thesis Submission

The following guidelines must be observed in all cases:

- The thesis should be saved as a PDF file and should be the same version as submitted to the College Research Degrees Board
- The file name should be the author's name (surname first), subject area and month and year e.g. Smith, Jane – Psychology – November 2015

If you thesis contains confidential or sensitive material, or it is under embargo or other restrictions please give details below.

Your Name (required)

Nasreen Ahmed

Your Student ID (required)

AHM16663573

Your Email Address (required)

16663573@students.lincoln.ac.uk

Your Thesis Title (required)

Building Better Biosensors Controlling the Surface Density of Probe Molecules on Glassy Carbon

Any details regarding confidential or sensitive material, restrictions or embargos

No

Please confirm the following statements that are applicable prior to submitting your thesis

☒ I am submitting the final version of my thesis as approved by the examining team. The content is the same as the fully bound version that will be submitted to the College Research Degrees Board

☒ My thesis **does not** contain any confidential or sensitive material that should be removed prior to publication

☐ My thesis **does** contain any confidential or sensitive material that should be removed prior to publication

☒ My thesis **does not** have any publication embargoes or restrictions

☐ My thesis **does** have any publication embargoes or restrictions

Submit your thesis and this form to your College Research Mailbox

College of Arts – collegeofArtsPGR@lincoln.ac.uk

College of Science – PGRCoS@lincoln.ac.uk

College of Social Science – cosspgr@lincoln.ac.uk

Lincoln International Business School – libspgr@lincoln.ac.uk

* Submitted theses will be made available via the University of Lincoln library/repository and the British Library unless otherwise notified

UNIVERSITY OF
LINCOLN

Building Better Biosensors

Controlling the Surface Density of Probe Molecules on Glassy Carbon

Nasreen Ahmed

Master by Research

University of Lincoln

2021

Acknowledgements

This work is dedicated to my father who devoted his life to me to maintain a dignified living, education and supported me to be resilient and the person I am today. Furthermore, I convey my sincere gratitude to Professor Steve Harding, Nottingham University who adopted my science journey in my earlier days in UK and supported and inspired the ambitious person in me to flourish.

In addition I would like to express my gratitude to my supervisors Dr Robert Johnson and Dr Tasnim Munshi who made my MSc possible. I would like to thank both of them for their consistent encouragement, motivation, patience and their sincere work and time they have spent with me throughout this Research Project. I am extremely grateful for accommodating, mentoring and inspiring my time in Lincoln.

In addition, I extend my thanks and appreciation to all the team members in the Chemistry and ICT Departments and my special thanks goes to Emma Jones. I would like to express my appreciation to Juliet Ibrahim, Nottingham University and Rachel Underwood, Sheffield Hallam University, Also, I am obliged to thank the Sheffield to Lincoln train services and train conductors who wake me up get off the train when I fell asleep and reminding me to check on my belongings when I leave the train.

Finally, I would like to confess to my children that you are my driving force; the care of Yasmien, the love of Nizar and last but not least the kindness of Khalid.

Table of Content

1. List of Abbreviations and Symbols

DNA	Deoxyribose nucleic acid
ssDNA	Single stranded DNA
dsDNA	Double stranded DNA
PCR	Polymerase chain reaction
SLP	Stem and Loop Probe
LP	Linear Probe
CV	Cyclic Voltammetry
CVs	Cyclic Voltammograms
Boc	tert-butyloxycarbonyl
V	Potential
i_p	Peak Current
Γ	Surface Density
GC	Glassy Carbon
NBD	Nitrobenzene Diazonium Tetrafluoroborate
BBD	Bromobenzene Diazonium Tetrafluoroborate
WE	Working Electrode
SCE	Saturated Calomel Electrode
RE	Reference Electrode

2. Abstract

Carboxylic-acid functionalized molecules can be immobilized into the surface of a glassy carbon electrode through a multi-step surface modification procedure in which nitrobenzene diazonium tetrafluoroborate is electrochemically grafted to the electrode surface and the NO_2 terminus subsequently converted to an NH_2 group that can readily be coupled via carbodiimide crosslinking. This surface modification has potential applications in the development of new electrochemical DNA biosensors when modification attest to be attainable and readily managed.

The aim of this study was to investigate the effects of changing the concentration of nitrobenzene diazonium tetrafluoroborate for the duration of the initial electrochemical grafting step on the surface density of the surface modification. To achieve aim, the diazonium modified glassy carbon surface was exposed to carboxylic-acid functionalized anthraquinone, the presence of which at the electrode is established by cyclic voltammetry and the magnitude of the signal record employed for the estimation the surface density of grafted molecules. Results from the study revealed that diazonium reduction can be used to prepare surface densities of anthraquinone on a glassy carbon electrode at circa 1×10^{12} molecules per cm^2, a value that is comparable to the surface densities of DNA probes used in current state-of the art electrochemical DNA biosensors on gold electrodes.

3. Introduction

3.1. Biosensors

Electrochemical Biosensors have developed rapidly in the last two decades. Some existing biosensors are commercial viable and used readily in clinical chemistry such as in health monitoring and diagnostics or industrial settings such as for agricultural and environmental monitoring.[1,2] The distinctive characteristics of electrochemical biosensors are the combination of sensitivity provided by an electroanalytical approach with the specific bio-selectivity of biological recognition sites. In particular, electrochemical DNA Biosensors for short nucleotides or nucleosides detection have progressed notably in recent years. The DNA sensing starts with formation of a self-assembled monolayer (SAM) of a probe single strand DNA (ssDNA) on the surface of a modified working electrode that only binds to the specific sites target of the DNA strand ssDNA to form a double dsDNA[3]. In clinical or biological samples, the DNA target which is available binds or hybridised to the probe DNA immobilised on the electrode. The electrochemical parameters are measured before and after the hybridisation process. Such measurements include changes in double layers capacitance, charge transfer through the DNA film *via* a solution based redox mediators, or electron transfer currents from a redox label that is bound to the probe sequence or target DNA.[4]

3.2. Biosensors Construction

The basic form of a biosensor consists of biorecognition sites, transducers and a signal processing device. The biorecognition sites works as a biochemical receptor or a component that utilises a biological interaction or selective binding to ascertain the presence of an analyte of interest, which can either be antibodies, enzymes and DNA.[5] The transducer works to transform the result of a biological interaction into a measurable output, such as a colour change or fluorescence or electrical current, which can be easily quantified. Figure 3.1 shows the fundamental principles of a biosensor[6]. In an electrochemical biosensor, the working electrode (WE) operates as a transducer and it can be made from a variety of conductive materials, such as gold,[7] platinum,[8] glassy carbon[9] and boron-doped diamond[9].

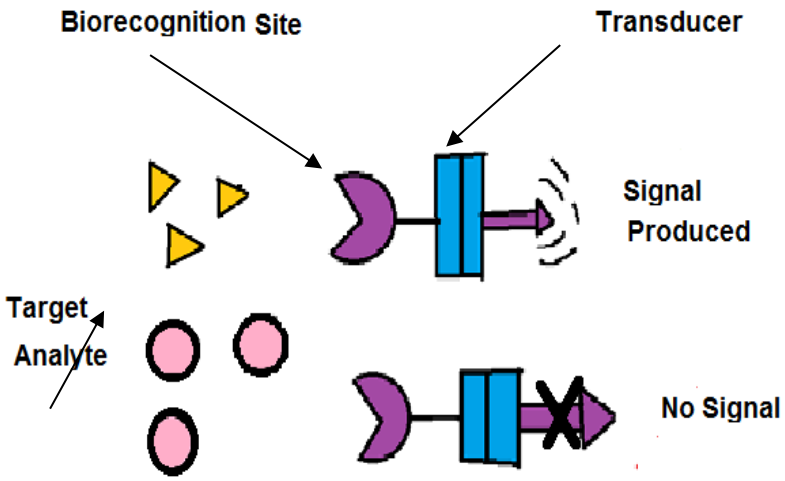

Figure 3.1. Diagram showing the basic functioning of a biosensor.

3.3. DNA Amplification and Bio-recognition sites

DNA structure consists of complimentary base pairing that has the ability to combine to form a double helix through annealing and dissociate through thermal de-annealing under specific conditions, Figure 3.2.[10] These natural characteristics have been employed as bio-recognition sites in biosensors.

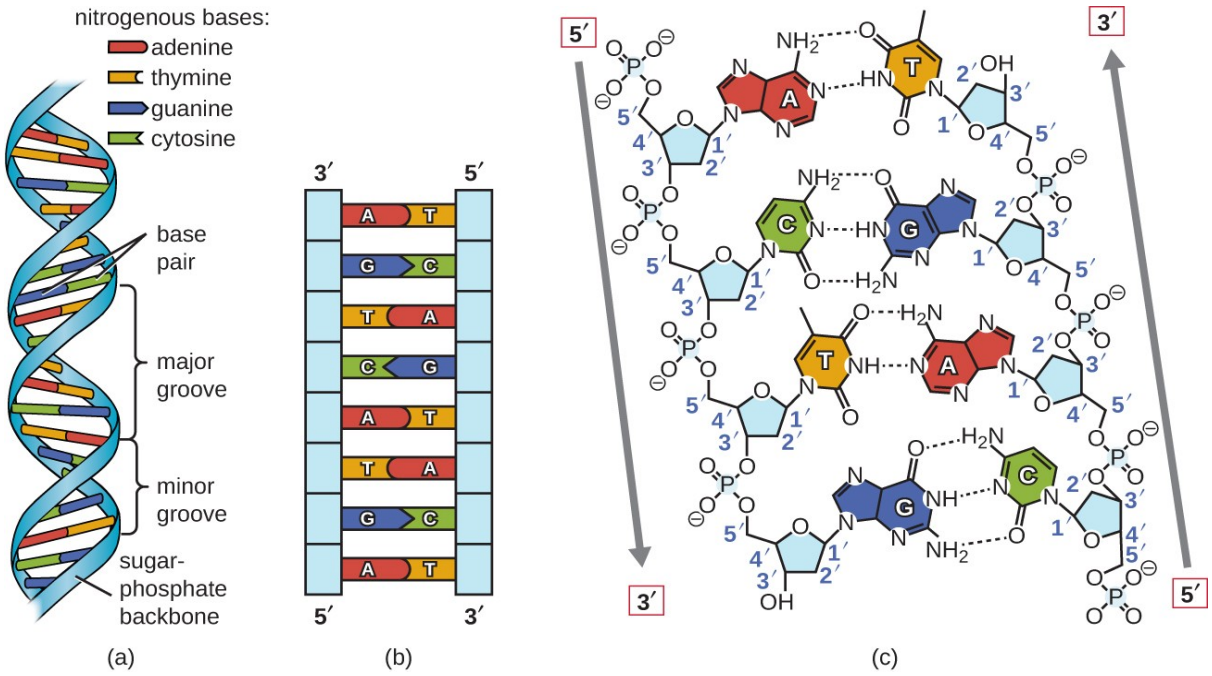

Figure 3.2. Diagram presenting the specific base-pairing in DNA, with the bases labelled (A = adenine, T = thymine, G = guanine and C = cytosine) and hydrogen bonding between the base pairs shown.[10]

DNA is a double helix of deoxyribonucleic acid made of two strands, bound together by hydrogen bonds between the two strands. Each strand contains mixed nitrogenous bases of adenine, thymine, guanine, and cytosine. Also, it contains a backbone comprising of phosphates and the sugar deoxyribose.

In most real-world applications, DNA must be extracted before it can be analysed with an electrochemical biosensor.[10] For example, in a medical setting, this may mean that a saliva or blood sample is to be taken. In such samples, it is usually the case the DNA is of too low concentration and in double-stranded form. To provide sufficient target molecules of single-stranded DNA for detection they first have to be generated by a Polymerase Chain Reaction (PCR) process. While PCR does not fall into the scope of the work carried out, in this project, it is briefly mentioned here due to its importance as the step immediately prior to that which has been investigated in this thesis, namely the detection of DNA targets that are the products of a PCR amplification reaction.

3.4. Electrochemistry

Electrochemistry involves electron transfer which leads to a chemical change. Cyclic voltammetry (CV) is one of the most important measuring and manipulation tools in

electrochemical DNA biosensors. Depending on of the information desired, various parameters can be applied. CV measurements require a working electrode (WE), reference and counter electrode (or CE). The Reference (Ag /AgCl) electrode maintains a desirable and stable potential. The CE works to complete the circuit with the electrolytic solution for the current that passes through WE, and the WE itself is the transducer element in biosensors where the biochemical reaction (in this case DNA hybridization) takes place.

When applying a potential in solution, the electron transfer may occur from the analyte to the electrode, or from the electrode to the analyte. The direction of the electrons (and hence current) can be controlled by applying an electrical potential (voltage) to the WE. Electrochemical biosensors measure the current produced by the oxidation and reduction reactions. The relationship between the concentrations of the oxidised and redox products at the surface of the electrode are linked to the potential is described by the Nernst equation:

$$E_{cell} = E^0 - \frac{RT}{zF} \ln \frac{(\mathrm{Red})}{(\mathrm{Ox})}$$

Where the cell potential, E_{cell}, is dependent on the standard half-cell reduction potential, E^e, at the temperature of interest, *T*, and the ratio of the concentrations of the oxidized (O_x) and reduced (Red) forms of the analyte in the system. The additional terms are, *z*, the number of the electrons transferred, Faraday's constant, *F*, and the universal gas constant, *R*.

The Nernst equation can provide a powerful measurement how the system reacts to change of the concentration of species in solution or a change in the electrode potential.[11]

While the potential of the peaks is dependent of the nature of the analyte, the measured current is dependent on the concentration (or specifically, for an immobilized species the surface density. The surface density, Γ, is related to the measured peak current, I_p, through the following equation:

$$i_p = \frac{n^2 F^2}{4RT} vA\Gamma$$

Where *n* is the number of electrons transferred, *F* is the faraday constant, *R* is the gas constant, *T* is the temperature, *v* is the scan rate and *A* is the area of the electrode.

3.5 Nucleic Acids Probe Biosensors

The architecture of DNA electrochemical biosensors has developed significantly over the past 20 years. The first generation of these types of sensor is the linear loop (LP) and stem and loop linear (SLP) , as shown in Figure 3.3.[12] In a LP sensor, the presence and binding of a target is indicated through a reduction in observed signal where the formation of a rigid DNA duplex holds the methylene blue probe far from the surface preventing electron transfer. This is unfavourable for electron transfer due to inflexibility of the probe-target and leads to significant reduction in redox current.[13] In the absence of the target, the methylene blue label is able to approach the surface through the flexibility of the single-stranded DNA probe.

In the SLP sensor, the methylene blue is rigidly held at the surface of the electrode in the absence of the target. When the target binds, the stem section, which is weakly bound, is displaced by the strongly-binding target, the methylene blue is held away from the surface and there is a significant attenuation in the measured signal. These sensors have been found to be susceptible to false-positive results and reduction in the redox signal. This could be due to monolayer degradation or non-specific adsorption of matrix contaminant.

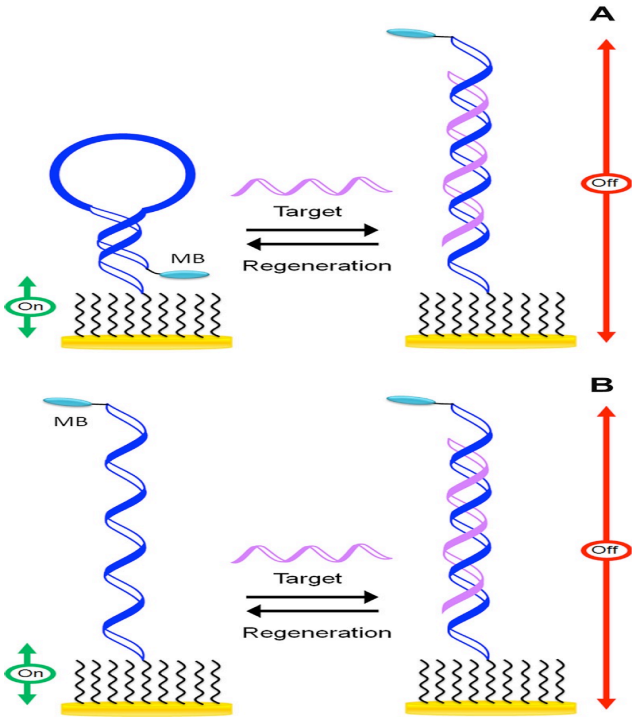

Figure 3.3. Diagram showing both SPL and LP signalling mechnisim in the absence and presence of a target.[12]

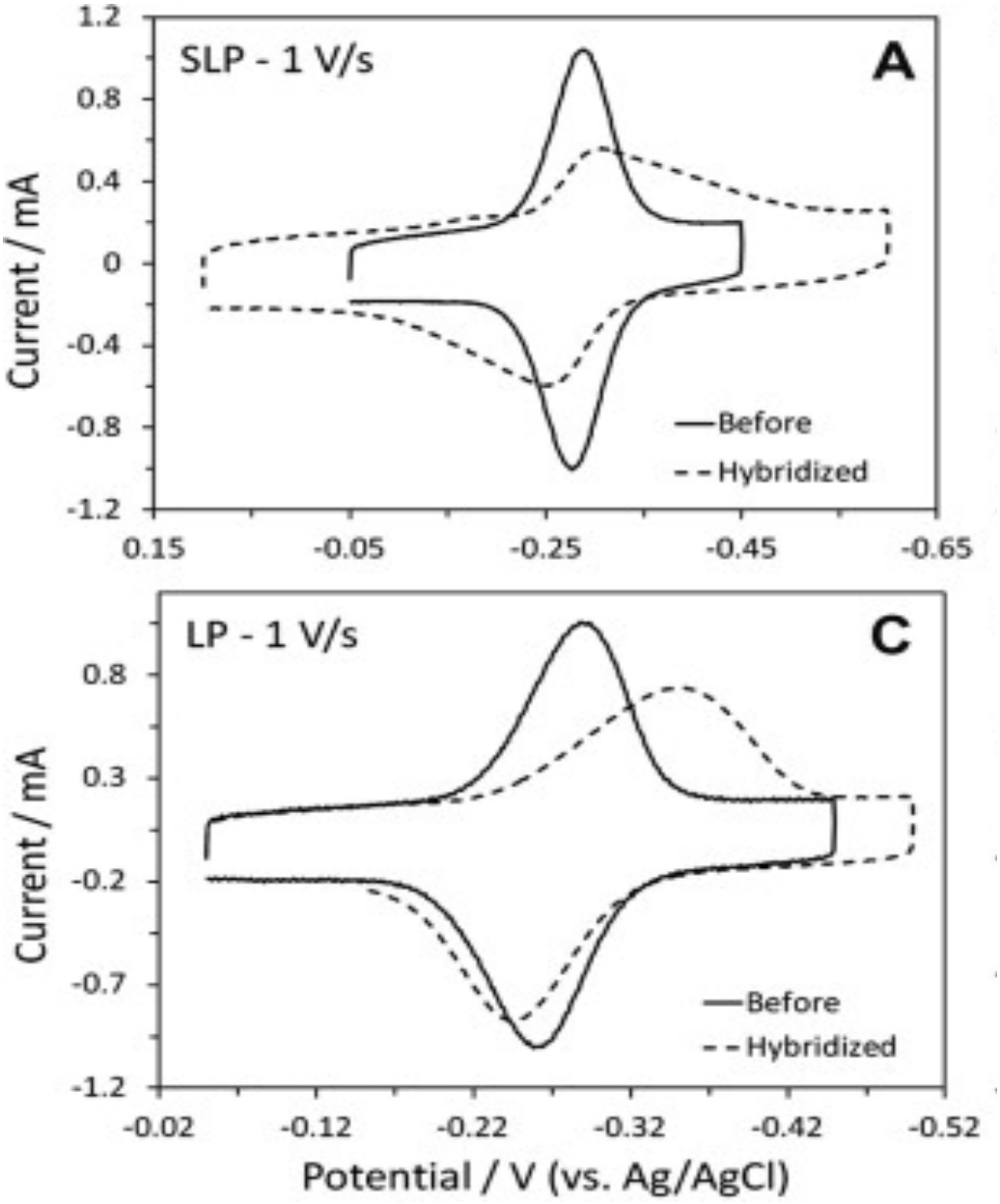

Figure 3.4. Illustration of the CV data produced by the first generation sensors stem linear loop (SLP) and linear probe and showing the decrease in the sensor response upon hybridization of a fully complentary target DNA.[12]

This limitations of these hybirdized probe sensors led to the developedment of second generation of “signal on” surface based electrochemical DNA biosensors. For these sensors, in the presence of the target the signal reponse also increases. These types of sensor employ more complex architectures,[14] as shown in Figure 3.5.

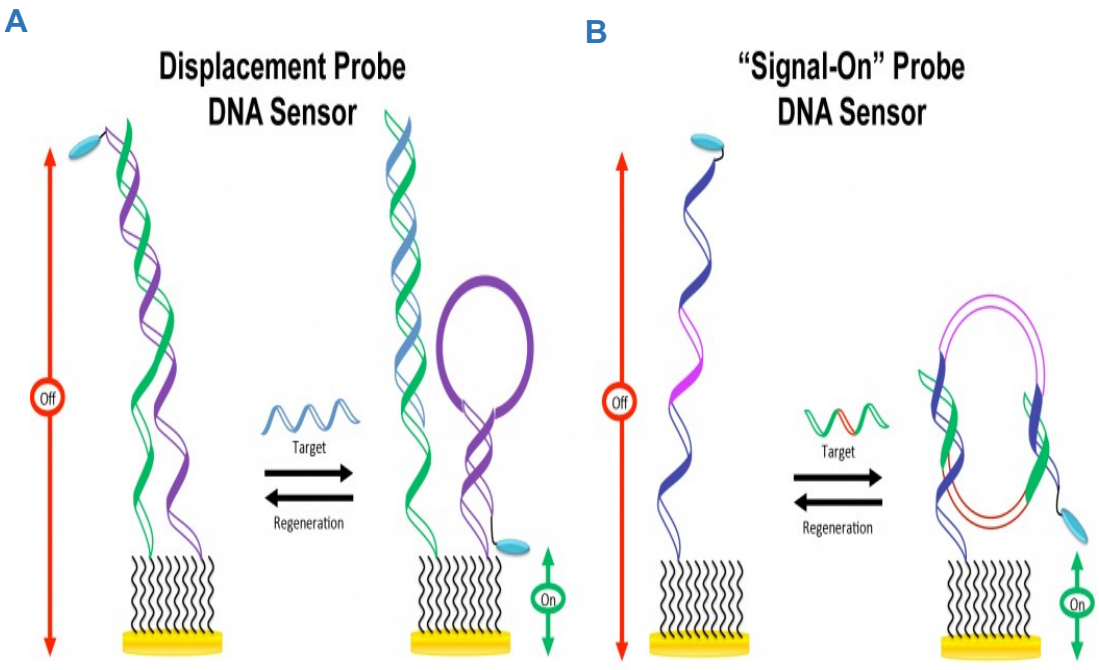

Figure 3.5 diagram showing the second generation of the surface-based electrochemical DNA biosensors that operate the signal on method by displacement (A) or cyclisation (B)[14]

3.6 Surface Immobilisation at Carbon Electrodes

Careful control of the surface density of the DNA probe in a biosensor is critical for optimal function. In cases where the surface density is too low, the concentration of the probe can be too low to generate the signal upon a binding event. Whereas if the surface density is too high, efficient binding to probe does not occur to produce the desired signal, Figure 3.6. Typically, a surface coverage of *circa* 1×10^{12} molecules per cm^2 is desired for optimal sensor performance.[15,14]

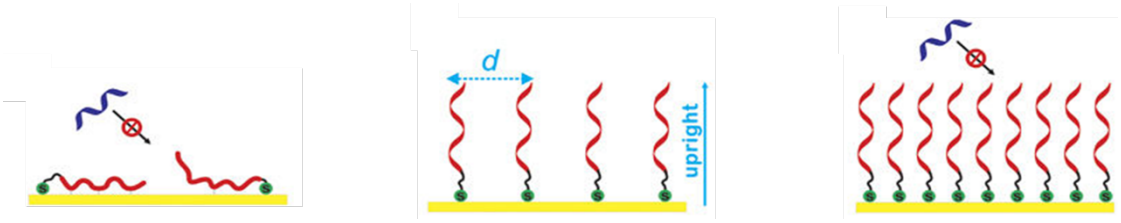

Figure 3.6. An optimal surface density is required for efficient hybridization of target to probe DNA in an electrochemical biosensor. [15,14,]

While methods to control surface density of DNA probes (such as for the architectures shown in Figures 3.4 and 3.5 on gold electrodes has been extensively explored, little is known about how to control surface density at carbon electrodes. As this thesis focuses on the use of diazonium salts to modify carbon electrodes, some recent approaches taken in this area from the recent literature are summarized below.

Formation of mixed layers of aryldiazonium salt: This is accomplished directly by electro-grafting by a one-step reduction. For example, a GC electrode was functionalised by both 4-carboxyphenyl and phenyl (1:1) mix in acetonitrile. However, it was found that the occurrence of multilayers could not be completely prevented, and this paper does not discuss the factors that influenced the surface ratio is addressed.[16]

Control over surface composition (binary-in-situ): The electro-composition of mixed monolayers of aryldiazonium salts of 4-NBD and 4-BBD on glassy carbon was explored for the first time by the Belanger group.[15] The 4-NBD is reduced more easily than 4-BBD at 0.2 V vs Ag/AgCl, regardless the ratio of the compounds in the solution.[17] The group precisely represented control of the composition of the electro-grafted layer by applying different reduction potentials at GC surface.[18]

Control over Spatial distribution: Thin films were created to attain different hybrid surfaces of binary aryl layers with control over the spatial distribution. Downard *et al.* created thin films of aryldiazonium salts that covalently attached to carbon electrode by the electrochemical reduction. Then part of the layer was removed with an AFM tip and a second component was attached on the uncovered surface are by the electro-grafting technique[19].

Control over structure of mixed layers: A few approaches for multi-layer growth prevention have been described. For example, controlling the experimental conditions such as viscosity of the solvent (replacing the organic solvents by ionic liquid, aryldiazonium salt concentration), applied potential or electrolysis time to allow mixed near-monolayer structure formation.[20,21] A mixed thin layer of 4-carboxyphenyl and phenyl moieties was functionalised on the GC electrode surfaces by Lui *et al*., this was achieved by reducing the electrodeposition times to only two cycling scans.[16] Furthermore, mixed monolayers prepared on gold and glassy carbon by reduction grafting when applying positive potential (approximately +2 V) have also been described. This was followed by oxidative electro-grafting at a negative potential[22] (approximately –1 V) for a second aryldiazonium, or by spontaneous grafting at open circuit potential[22]. Adding a chemical radical scavenger[23] has also proven successful in reducing the building up of branching layers effectively.

4. Aim and Objectives

The aim of this research is to modify and measure the surface density of a redox active anthraquinonoid (AQ) when bound to the surface a glassy carbon electrode by cyclic voltammetry. In this thesis, the anthraquinone acts as a cost-efficient stand-in to DNA, with the results expected to inform subsequent work on carboxylic-acid modified DNA probes.

Modification of glassy carbon electrodes with AQ is achieved by immobilising a nitro group onto the electrode surface using the salt 4-nitrbenzene diazonium tetrafluoroborate (NBD). Part of the research is to determine how the surface density of the immobilized anthraquinone molecules are affected by the concentration of NBD used during the grafting process. The objective is to produce surface densities of AQ-NH-benzene at circa 1×10^{12} molecules per cm^2, analogous of desirable surface density of DNA probe biosensors.

5. Experimental

5.1 Chemical and Equipment.

Table 5.1 Equipment used and source

Equipment	Source
Glassy Carbon [Working Electrode]	Biologic Inc
[Working Electrode]	
Saturated Calomel Electrode (SCE)	IJ Cambria
[Reference Electrode]	
0.5 mm Platinum Wire	Alfa Aesar
[Counter Electrode]	
EmStat^3 Potentiostat	PalmSensBV
MicroCloth Polishing Cloth	Buehler
CabriMet S Silicon Carbide Abrasive Paper	Buehler

Table 5.2 Software used and developers

Software	Developer
PSTrace 5	PalmSensBV
[EmStat^3 Potentiostat]	
Excel	Microsoft
Origin 2017	OriginLab

Table 5.3 Chemicals, abbreviated name and suppliers

Chemical	Abbreviation	Supplier
Alumina Powder (1μm)	-	Buehler
Acetonitrile	Acetonitrile	MERCK
Tetrabutylammonium tetrafluoroborate.	TBATF	MERCK
4-Nitrobenzenediazonium tetrafluoroborate	NBD	MERCK
N-Hydroxysuccinimide	NHS	Alfa Aesar
N-(3-Dimethlaminopropyl)-N'-ethyl carbodiimide Hydrochloride.	EDC	MERCK
N,N-Dimethylformamide	DMF	MERCK
Potassium Nitrate	-	MERCK
N-Ethyldiisopropylamine	DIPEA, DIEA	Alfa Aesar
Anthraquinonoid	AQ	Alfa Aesar

5.2. Electrochemistry Experiment preparation

All three electrodes the glassy carbon, reference and the platinum wire counter mentioned in Table 3, are used in each stage of the electrochemical experiments. This was after each electrode was cleaned appropriately according to the protocols followed in section 5.3. Subsequently, 5 -10 ml of the electrolyte sample of interest was placed into a 25 ml beaker. The three electrodes were dipped inside the solution by about 2 -3 cm, as shown in Figure 5.1.

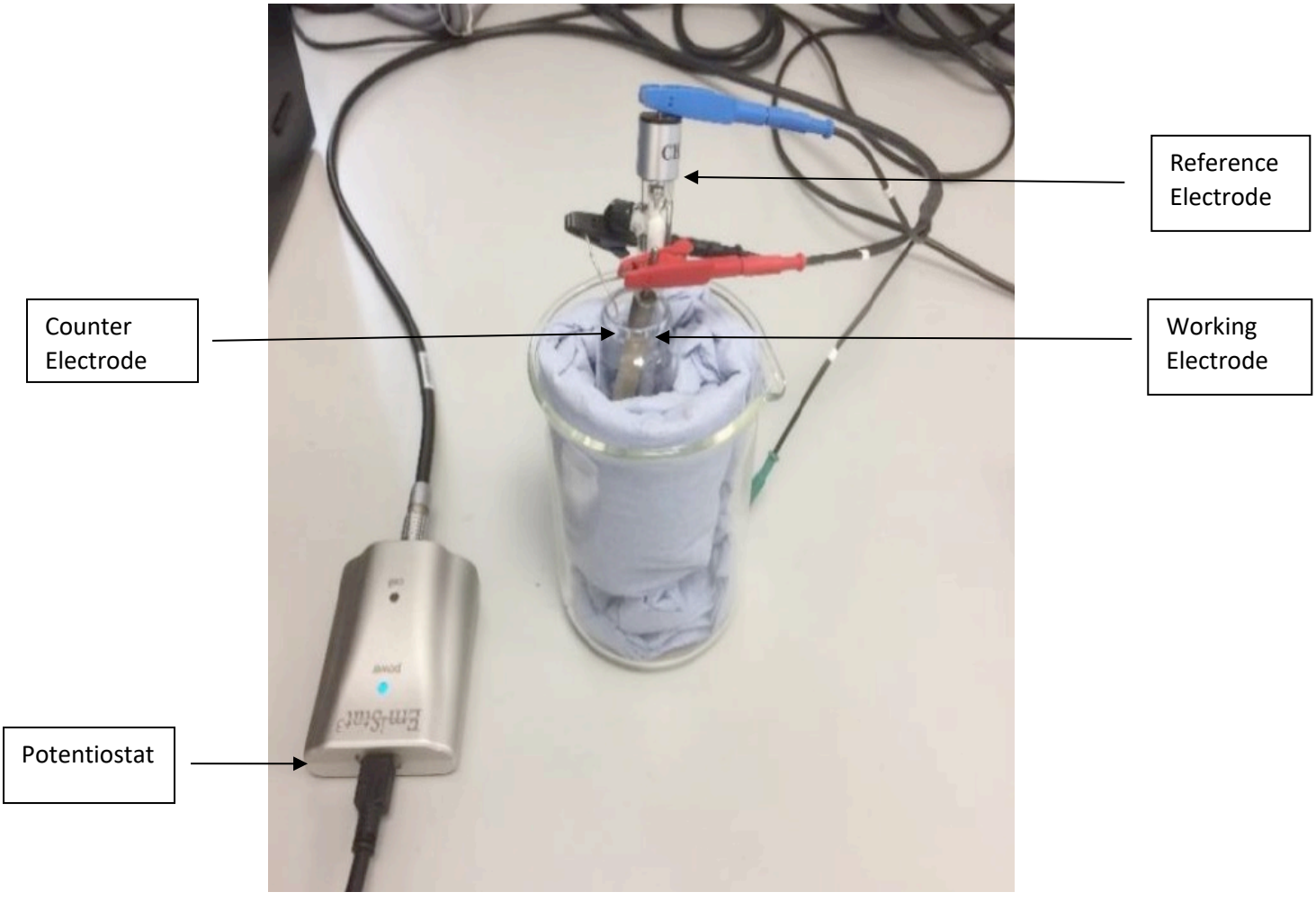

Figure 5.1 Diagram showing the setup of an electrochemical experiment.

5.3. Cleaning and Polishing Electrodes Procedures

Electrodes to be utilised were cleaned before commencing with each experiment. The reference electrode was washed with distilled water. Whereas the platinum counter electrode was rinsed first with water and then sterilised by a blowtorch flame for approximately a minute. The working Glassy Carbon (GC) electrode was cleaned using mechanical methods. This mechanical cleaning was carried out by polishing the GC electrode on the silicon carbide paper of grain size 200 mm. This step was followed by washing with distilled water before another polishing process in which a small amount (1g) of 1 μm alumina powder and 1 ml of water which was used to form a slurry on Microcloth on which the electrode is polished to consistent finish. Immediately prior to use, the GC electrode was washed with water to remove any excess of the alumina powder.

5.4. Data Analysis

PSTrace5 (Alvatech Ltd) software was used to analyse the recorded data produced by the Cyclic Voltammetry. The current and peak were defined by using the fixed baseline function. The appropriate scan rate and current peaks for the calculation process were selected from the four scans of each experiments, with reading of the first sweep was excluded due to double-layer charging effects.

The software Origin was used to calculate the gradients and R2 values for each collected voltammograms data for all experiments. Also, Origin was used to compare data produced by cyclic voltammetry. EXCEL programme was used to calculate GC surface coverages and error values.

5.5. Immobilisation and Reduction of the Nitrobenzene Diazonium

A solution containing nitrobenzene diazonium tetrafluoroborate was dissolved in 10 ml of acetonitrile containing 0.1 M TBATF. The selected voltage of the NBD immobilisation procedure was 0.6V to -1 V at scan rate of 0.05 V S^{-1} for 5 scans. This study was carried out for five various concentrations of 1.0, 2.5, 5.0, 10, 20, 40 mmol of NBD samples. Following the immobilisation step, the working electrode was washed with acetonitrile followed by distilled water and the electrode was placed in a 25 ml beaker containing 0.1 M KNO_3 solution. The applied voltage was swept from 0.2 to – 1.5 at a 0.5 V S^{-1} scan rate, to facilitate the reduction process of the immobilised NBD.

5.6. Evaluation of the GC Surface Density

5.6.1 GC Anthraquinone Modification Process

A mix of 0.00575 EDC, N-hydroxysuccinimide 0.2 M solution, 150 µl AQ-COOH 0.1 M solution, 30 µl of 0.1 N-ethyldiisopropylamine and 30 µl of DMF were allocated into Eppendorf tube. The working electrode was placed inside the tube with the mixture above after washing with DMF. These were sealed with a rubber tape and left overnight for *circa* =16 hours.

5.6.2 GC Modified Anthraquinone Data Collection.

In this experiment the anthraquinone was prepared in 0.1 M TBAF solution and added to five different concentrations of NBD as mentioned in the Experimental section. The Figures 6.5, 6.8, 6.9, 6.10. 6.11, 6.12 are graphs that produced by the addition of the Anthraquinone to 1, 2.5, 5, 20, 40 mmol of NBD. Electrochemical CVs of SR; 01, 0.25, 05, 0.75, 1.0, 2.5 Vs^{-1} have been performed for each of the above concentrations.

6. Results and Discussion

6.1. Immobilisation of the 4-NBD to the GC surfaces

4-Nitrobenzene diazonium tetra fluoroborate salt (NBD), prepared in various concentrations were immobilised as shown in Figure 6.1 and attached to GC electrode surface using cyclic voltammetry. This step is achieved by applying a negative potential from 0.6 to – 0.1 V at scan rate 0.05 V s^{-1} for 5 scans, shows of the cyclic voltammogram Figure 6.2.

Under these electrochemical conditions the diazonium loses two nitrogen atoms and forms a radical aryl cation, and subsequently a C-C covalently bond can be created, as illustrated in Figure 6.1. The typical characteristic NBD diagram is represented by the first scan that significantly shows the largest peak compared to the later scans that follow. This proves that the NBD salt reduction process has taken place.

These peaks are not observed on the 2nd and later scans, suggesting that the electron transferred has been inhibited from the electrode to the nitrophenyl groups. This is due to the complete reduction of NBD at the surface of electrode, which prevents the diffusion of further NBD molecules to the carbon electrode surface[24].

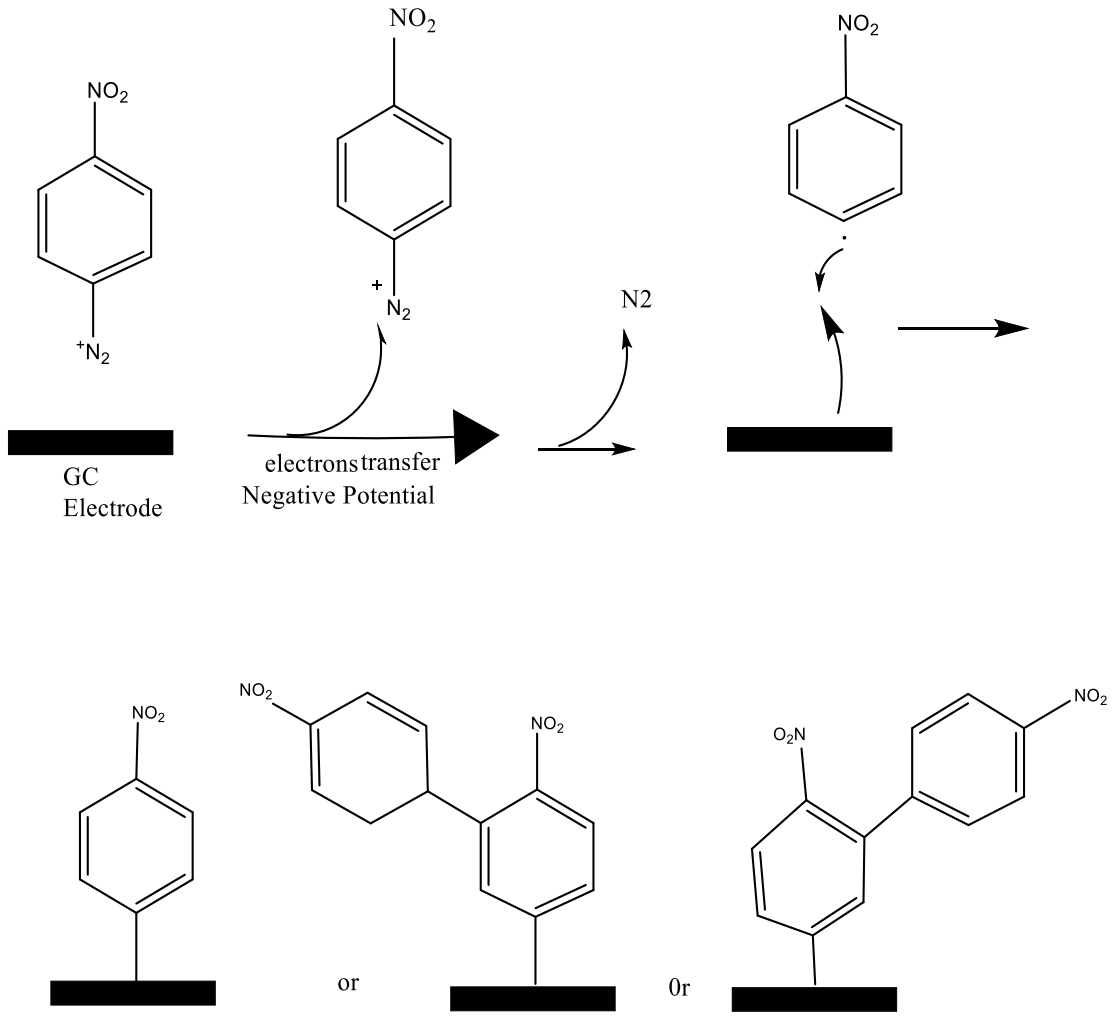

Figure 6.1 Diagram shows the electrochemical – initiated of the NBD attached to the GC surfaces and possible monolayer and multilayers branching formation.

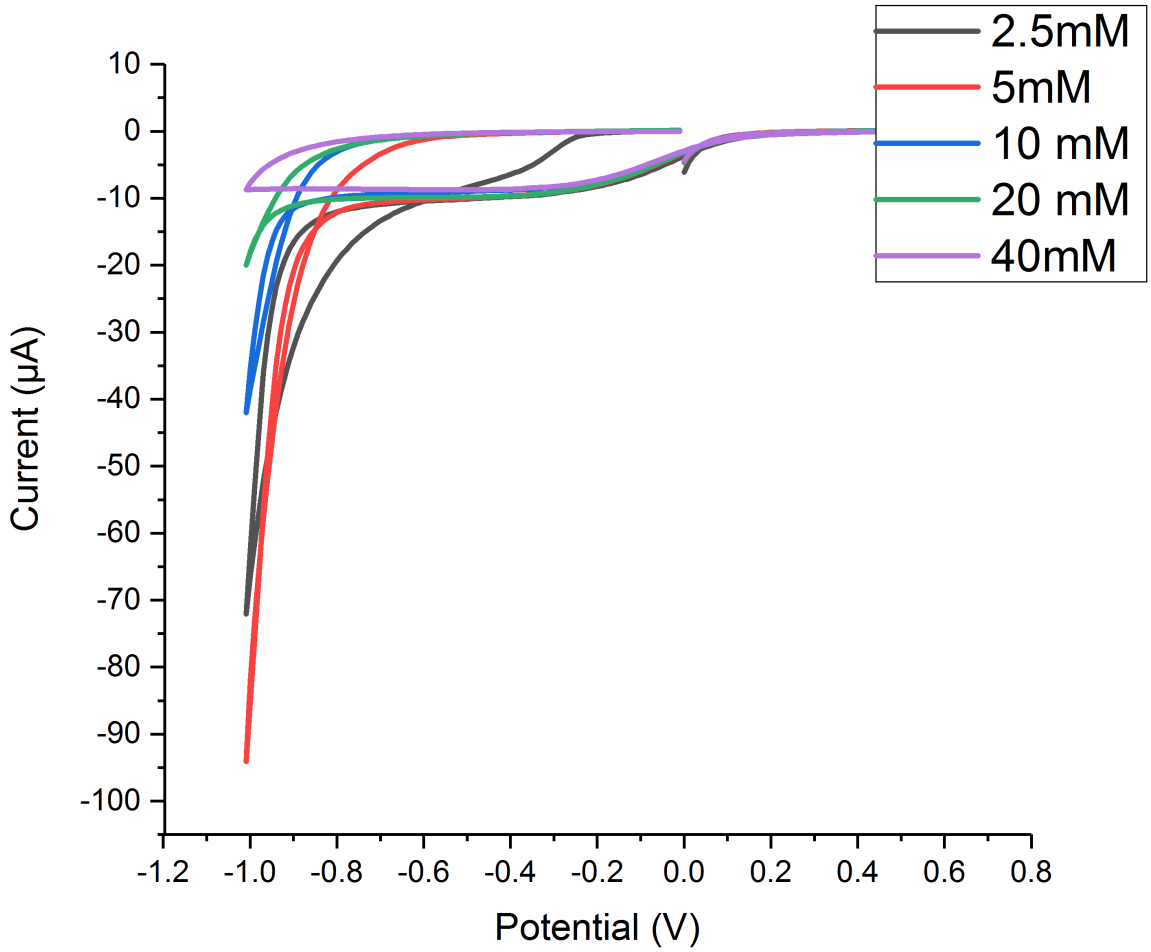

Figure 6.2 Graph shows the 1st scan of GC immobilisation BND curves produced by (2.5, 5, 10, 20) mM, SR 0.05 V^{-1} and the applying potential is (0.6 -).

The present voltammogram graph recorded is shifted slightly towards more negative than -1 for the lower concentration peaks, respectively. The graphs shows a larger dip reduction peaks at higher concentration correspondingly, verified between less 0.6 and more than -1.2 for the all tested concentrations.

During the grafting of NBD to the glassy carbon surface when lower concentration solutions of NBD are used (e.g. 1 mmol, Figure 6.3), a dissimilar shape cyclic voltammogram is detected. This because the potential is scanned negative, the conforming increases in reductive current is smaller than expected. In addition, the return cycle the voltage-current trace overlaps itself. This suggests the surface area is changing during the grafting reaction.[25] We speculate that the ACN solvent used for the reaction contains impurities that compete with the NBD for sites of the GC electrode surface. Thus, at lower NBD concentrations like that in Figure 6.3, the impurities begin to affect the observed current-voltage response[26].

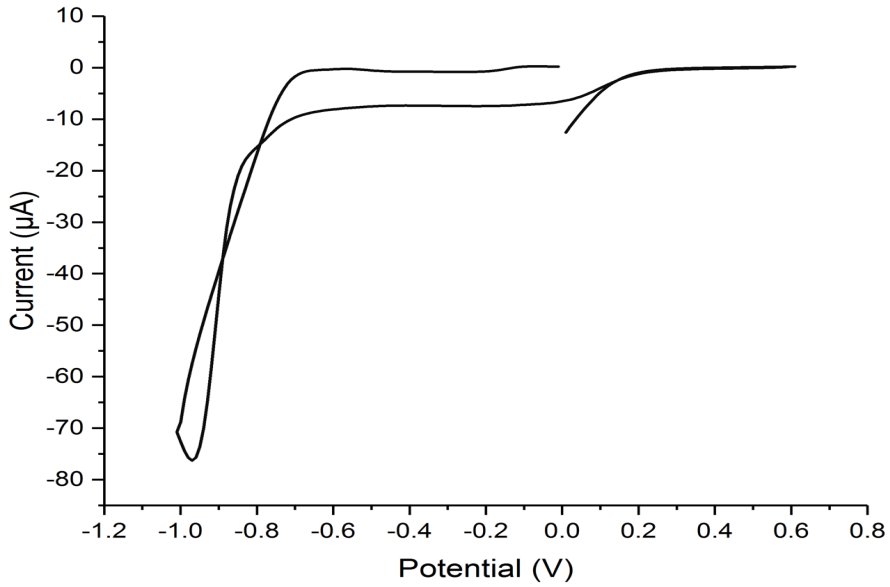

Figure 6.3 Graph shows the 1st scan of GC immobilisation BND (1mM), SR 0.05 V^{-1}
Note: the curve shape is unlike the higher concentration curves produced by (2.5, 5, 10, 20, 40) mM.

6.2. Electrochemical Reduction of Nitrobenzene NBD to an Amine

Upon establishing the immobilisation of the nitrobenzene on the GC surfaces, the following stage was electrochemically reduce the nitro group of NBD to an amine. This was accomplished by applying additional negative potential of (-1.5V – 0.2) at the surface of an electrode, dipped in KNO_3 solution. This demonstrates the cyclic voltammogram in Figure 6.4.

There are evident severe peaks observed in the first reduction cycle, sweep for the all diverse concentration studies, in all circumstances the disappearance of the main peak on subsequent cycles was observed due to the complete reduction reactions of NO_2 to the targeted NH_2 amine groups.

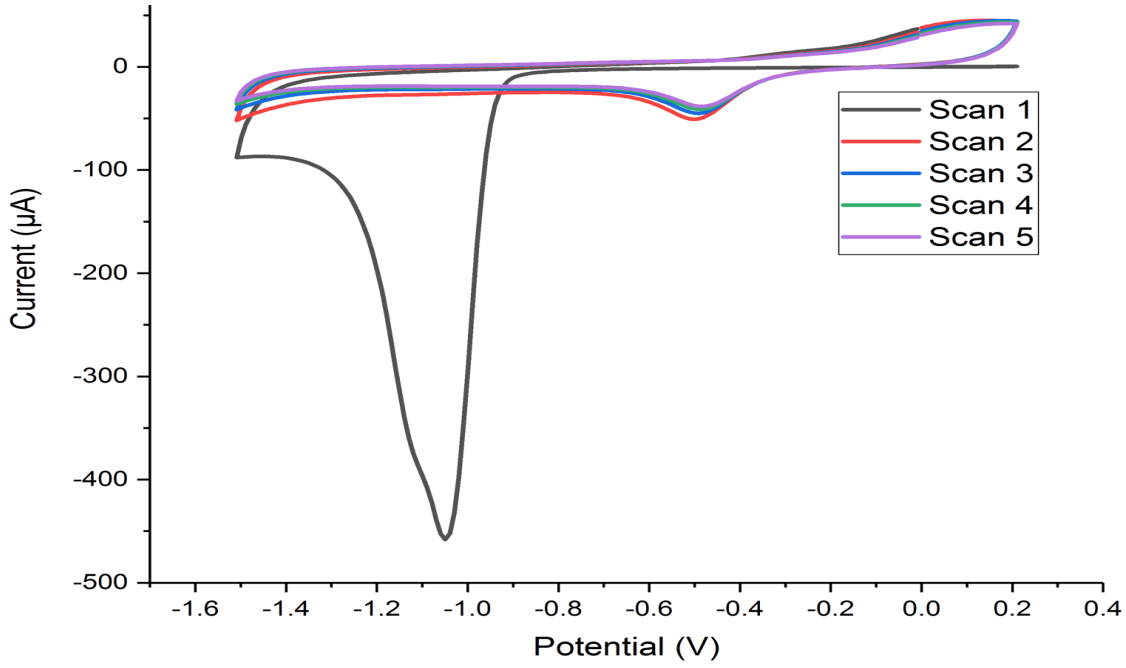

Figure 6.4 CVs of (scan rate 0.05 Vs^{-1}, 5 scans) produced sharp peaks as a result of converting the nitro group of the immobilised NBD on the GC electrode surface to an amine group.

As the potential is scanned negative, 2 peaks are detected. The first peak was attributed to the reduction of oxyen-contaning groups present on the electrode surface, that are known to form when the glassy carbon is exposed to the atmopshere[27]. The second peak which is between -1 and -1.2, was owing to the reduction of the NBD and the preceding formation of the grafted surface layer. The nitro nitrobenzene multi-layers fuctionlized and reduced to analines. However, it may take longer for the process to be completed, because they are alocated away from the elctrode surface., thus the electron transfer would take longer to occur.[28]

6.3. Electrochemistry of Coupling Modified Reaction of GC Electrodes and the Redox-active Anthraquinonoid

Following the NBD immmoblisation and the NO_2 reduction facilitating step, anthaquione was bound to the surface immoblised aryl-diamzoum as descrbed in the epexerimental section 5.3. The reaction occurs on multi steps as illustrated in Figure 6.5. Cyclic voltametry of the surface-bound anthraquione was then recorded, the AQ voltammogram shows two peaks,[29] one for the anodic reduction and one for the cathodic oxidation process on the surfaces, Figure 6.6. The existence of the oxidation and reduction peaks demonstrates that the reaction is reversible. The reaction was studied before and evidenced to be a reversible oxidation and reduction reaction involving 2 protons and 2 electrons.

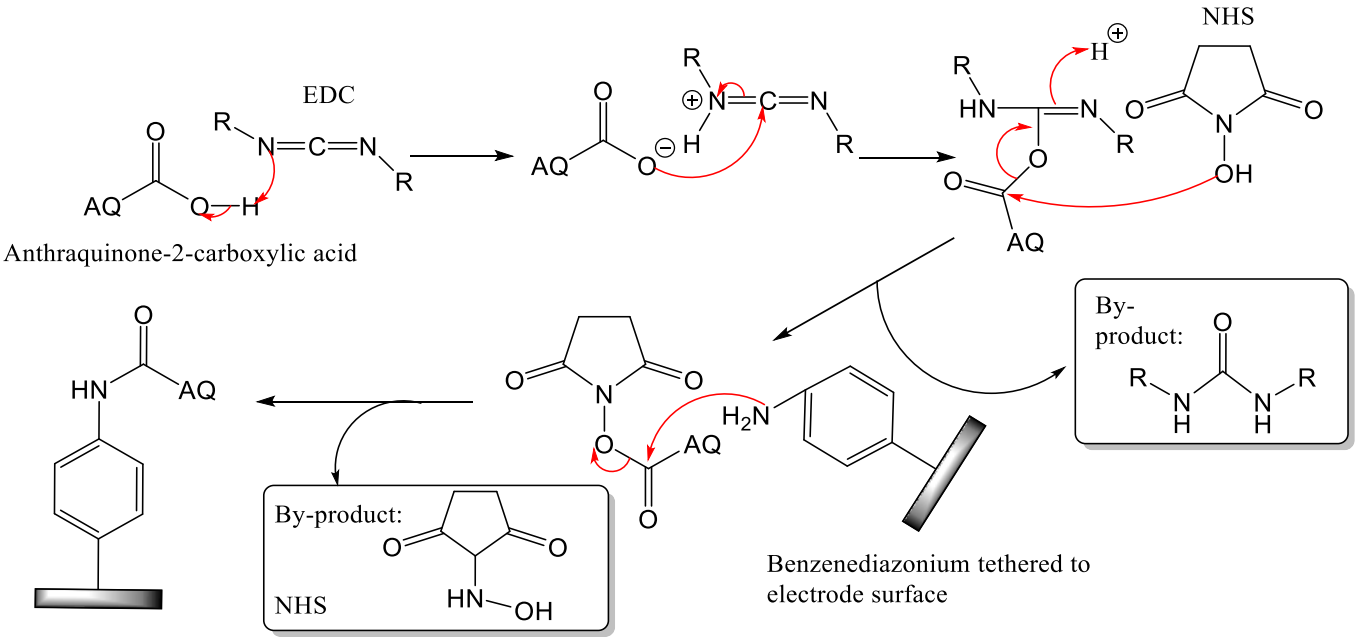

Figure 6.5 Reaction diagram illustrates the steps mechanisim of amide bond formation between the immoblised alanine and anthraquinone carboxylic acid, facilitated by 1-(3-dimethlaminopropyl)-3 - ethyl carbodiimide hydrochloride (EDC) and N-hydroxysuccinimide (NHS).[30, 31]

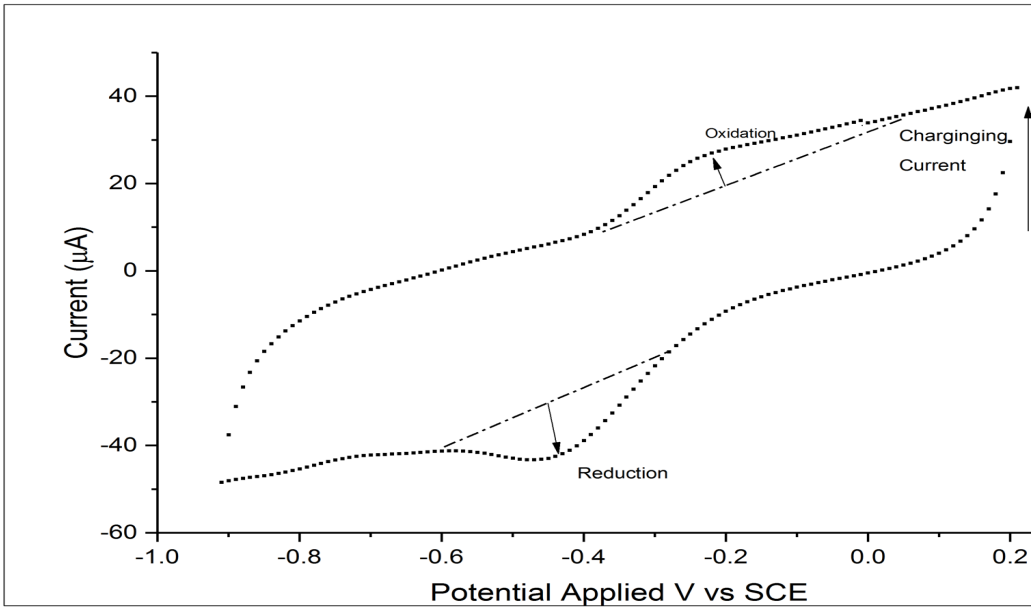

Figure 6.6 CV voltammgram obtained from Glassy carbon Electrodes fuctionlized 20 mM NBD - AQ mM NBD at Scan Rates 1.0 Vs^{-1} (V vs SCE). Shows the charging current, baseline of the both oxidation and reduction peaks.[29]

The peak at -0.6 ~ -0.7 in AQ component produced as a result of the solvated oxygen in the solution which maybe the peroxl and hydroxyl radicals however more tests are needed to confirm these species.[32, 33] This is in agreement with hydrodynamic studies of oxgen reduction rection (ORR) on modified monohydroxy anthraquinone (MHAQ) MHAQ/GC and MWCNTs/GC occurance on more negative than -0.4 or at -0.5.[34] The third peak could be due to any species compounds products since it occurs before or more negative potential value of the oxygen activitiey of these electrodes.[35]

The results match well with previous research with deposition of AQ with grafted diazonium salt in ACN.[36], in addition, to the expasion of the peak potential height and their magnitudes by increasing the aggregate concentration of NBD. The magnitudes or the width of peak increases when the concentration increase due to excess presence of anions and cations counterions near the electrodes.[37] Afterward, an increase in seperation capacitance background charging current. Whereas at the highest scan rate (2.5 and 5) Vs^{-1} the magnitude of both oxidation and reduction increases appears very short or undistinguished height.

Nevertheless, the wide magnitudes and smaller peak height that appear with higher scan rates suggests either poor coupling or indication of a dissimilar chemical reaction. This can

be explained by the multilayers formed during the primary immobilisation reaction explained in section 6.1. The branches of the multilayers prevent the AQ to reach the GC electrode surface or can be buried away from the surface and not easily bind to the AQ.[35] For that reason, multi graphs of the peaks height verse the SC as in Figure 6.7 was used to produce the estimated values of the surfaces coverage concentrations (Γ'_{sur}) for the oxidation and the reduction process. The mathematical methods have been applied for all NBD concentration (1, 2.5, 5.0, 10, 20, 40 mM), as showing in Figures 6.8 – 6.12.

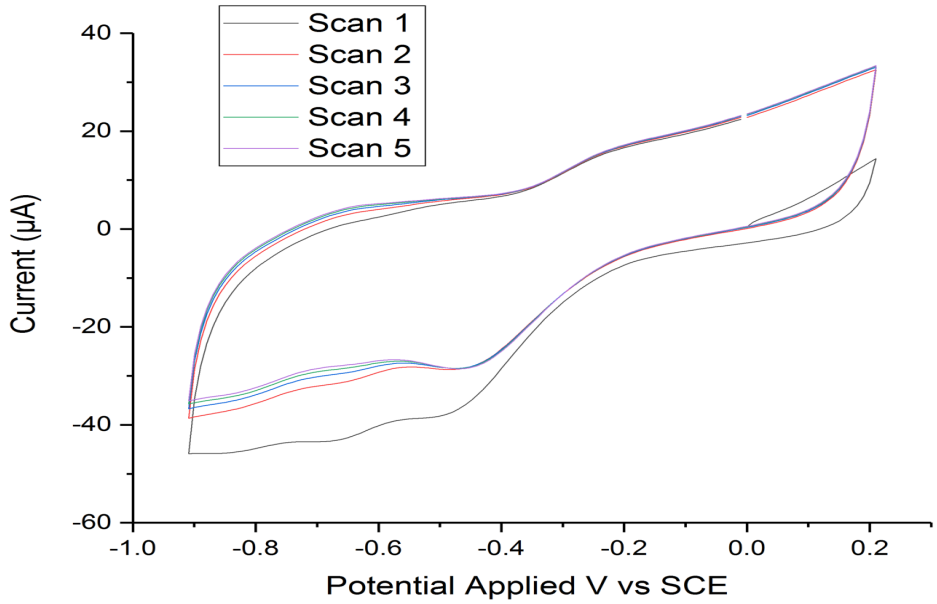

Figure 6.7 CVs obtained from GC modified 10 mM NBD electrodes, at scan rate 1.0 Vs^{-1} for 5 scan cycles to show changes in peak current that occur with each scan.

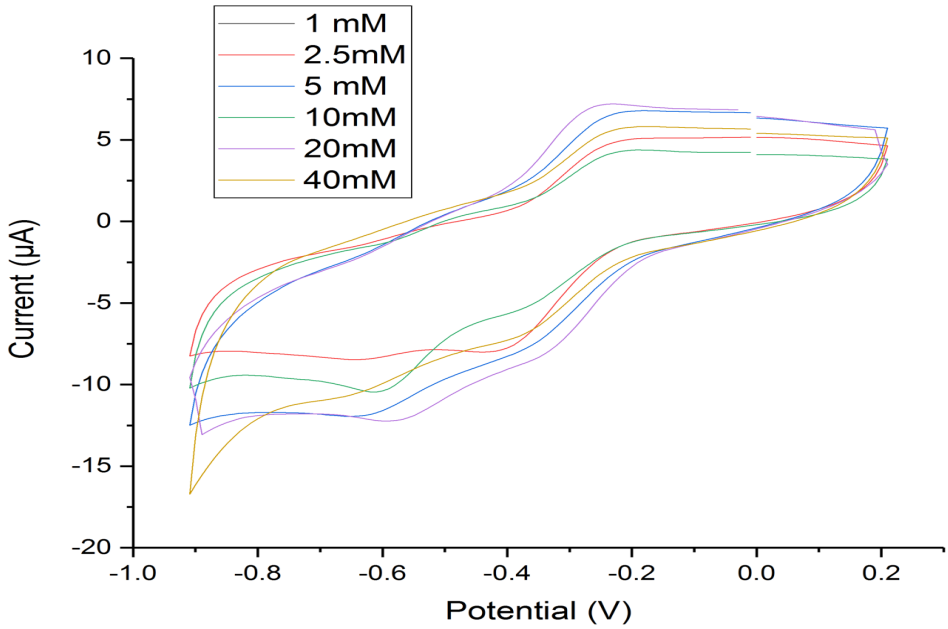

Figure 6.8 Stacked plots of CV Obtained from Glassy carbon Electrodes modiefied with (1, 2.5, 5,10, 20 and 40) mM NBD at Scan Rates 0.1 Vs^{-1}.

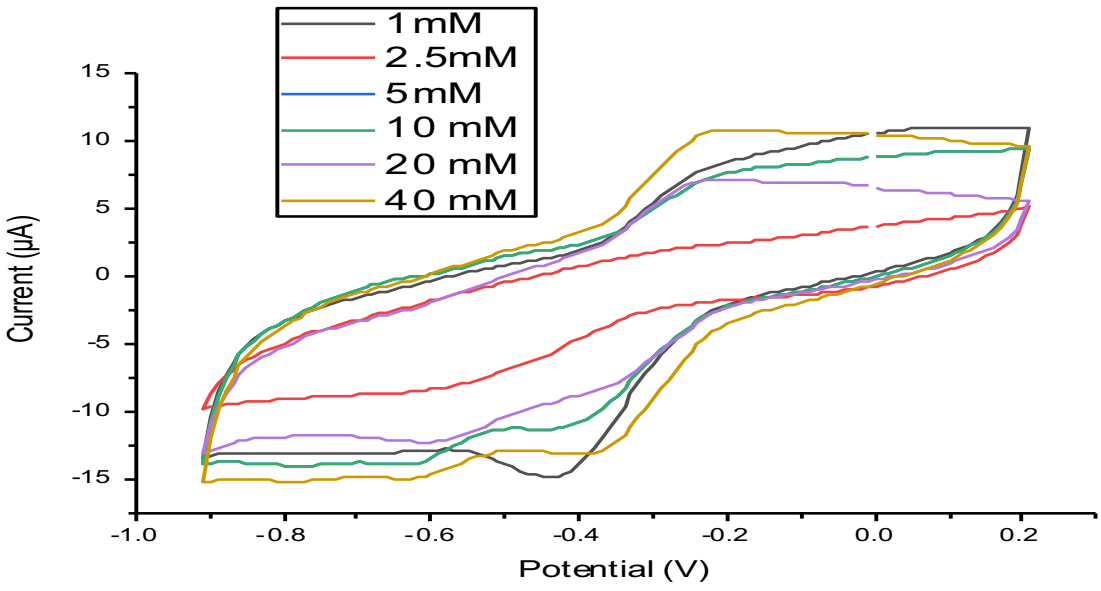

Figure 6.9 Stacked plots of CV Obtained from Glassy carbon Electrodes modiefied with (1, 2.5, 5,10, 20 and 40) mM NBD at Scan Rates 0.25 Vs^{-1}. Note: The data 2.5 mM at scan rate 0.5 Vs^{-1} is missing.

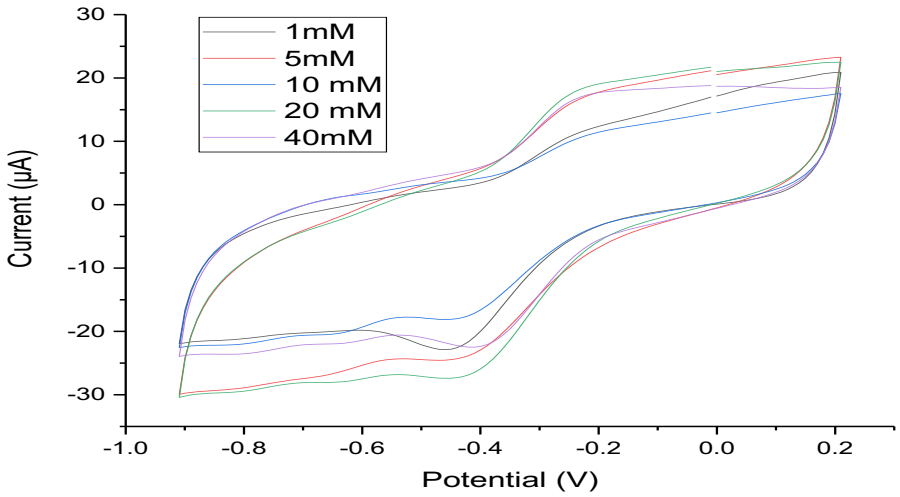

Figure 6.10 Stacked plots of CV Obtained from Glassy carbon Electrodes modiefied with (1, 2.5, 5,10,, 20 and 40) mM NBD at Scan Rates 0.5 Vs^{-1}.

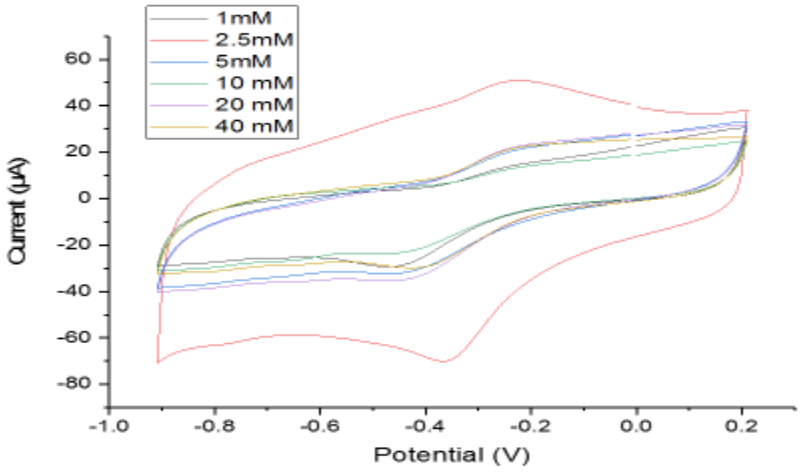

Figure (6.11) Stacked plots of CV Obtained from Glassy carbon Electrodes modiefied with (1, 2.5, 5,10,, 20 and 40) mM NBD at Scan Rates 0.75 Vs^{-1}.

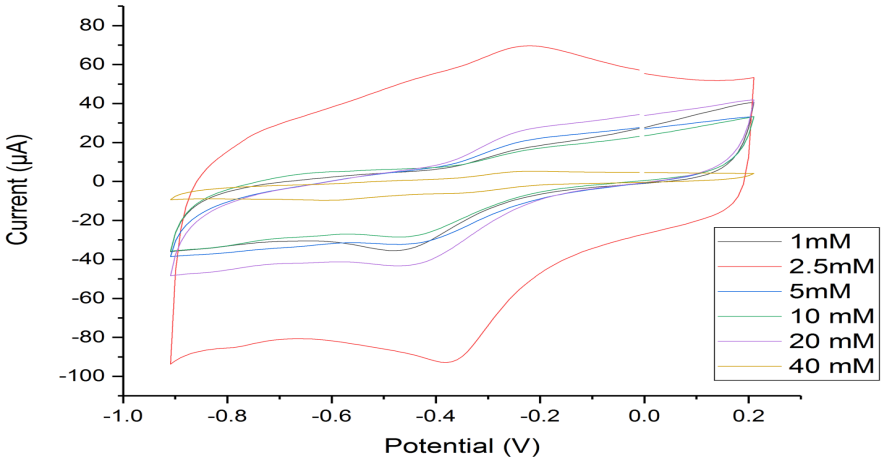

Figure 6.12 Stacked plots of CV Obtained from Glassy carbon Electrodes modiefied with (1, 2.5, 5,10,20 and 40) mM NBD at Scan Rates 1.0 Vs^{-1}.

Note: At scan rate 2.5 Vs^{-1}, there are no significant peaks found of most concetration.

6.4. The Surface Covarage and the Surface Density.

The establishment of the anthraquinoniod attached to GC via the analine group displays a linear relationship between scan rates and the applied faradaric current, which is presented by the'peak height', Figure 6.13 make available successful results confirmation for this modification[38]. The oxidation and reduction survace coverage (SC) concentration Γ'_{conc} is calculated from the P_{height} *vs* SR plots for each experiment. This produces strong linearity relationship between scan rates and peaks hights. Thus the slope of the line can be substituted in equation (1) to establish the survace coverages Γ'_{conc} values in mole.cm-^{2}.

Surface Coverage $\Gamma'_{conc.}$ = m4RT /e^2F^2Ar^2 π ⟶ equation 1

R is the universal gas constant, n is the number of electrons, and T is the temperature.

After the SC have been calculated, additional measurement of the amount of the deposite reducted NBD on the GC surface can be calculed in molecular cm^{-2} (Γ'_{area}) as shown in Table

6.1. Based on equation (2). These values signify the exisitng AQ molecules binding to the targeted NH_2 function group in one cm^2 on the GC surfaces.

Surface Coverage Γ'_{area} = SC ($\Gamma'_{conc.}$) × $6.022*10^{23}$ ⟶ equation 2

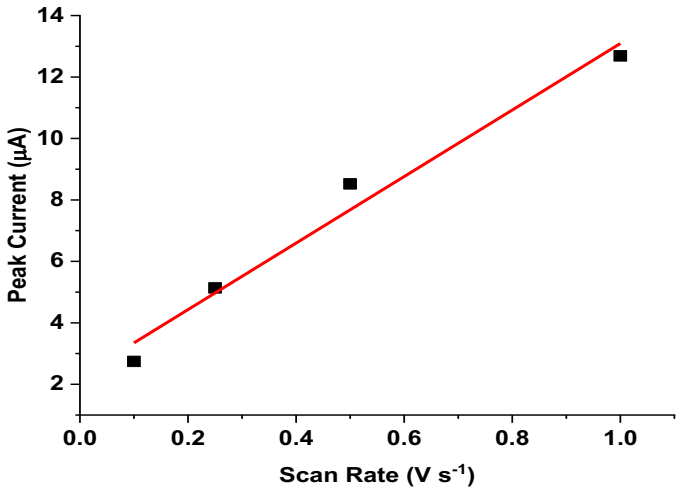

Figure 6.13 Graph explaining linear correlation between scan rate and peak hight on GC electrode modified with 20 mM NBD. The error for the peak current, taken from the noise in the CV signal was calculated to be negligible and considered no error in scan rate

Table 6.1 Surface coverage area evaluation

Nitrobenzene Concentration (mM)	**Γ' Oxidation Peak (× 10^13 molecules cm^{-2})**	**Γ' Reduction Peak (× 10^13 molecules cm^{-2})**
40	2.5 ± 0.25	1.3 ± .02
20	2.4 ± 0.26	2.5 ± .07
10	1.79 ± 0.07	1.1± 3.3
5	0.04 ± 0.012	0.04 ± 0.01
2.5	0.008 ± 0.002	0.011 ± 0.0011
1	0.013 ± 0.000	0.02 ± 0.006

Acording to Table 6.1 an intensification in SC with further increase in concentration of NBD was observed. However, this is not the case in all the comparison CV graphs diagram for each SR values for the 1 mM NBD concentration due to the impurity as discussed previously

in section 6.2. Adam *et al* have composed that the species concentration and the peak current that is transported electrochemically to the electrode in votammetry, are proportional to its concentration in the solution.[39] While the established SC data are dependent on the geometrical area of the GC electrode. While, the established of SC data are dependent on the geometrical area of the GC electrode, a surface coverage needs other methods to confirm the thickness of the layer, such as Raman spectroscopy, *X*-ray photoelectron spectroscopy (XPS) or atomic force microscopy (AFM).

Comparing the result in Table 6.1 with other studies, the electrode surface roughness factor with layer thickness electrochemical deposit in GC for the same modifier NBD salt. The roughness factor between 1.5 to 2.5 was discovered for a polished GC produce monolayer of (18 – 30) × 10^{-10} mol cm^{-2} of the geometrical surface.[40,]

This is well matched to the SC result produced by 2.5 and 5 mM of NBD concertration Table 6.1.

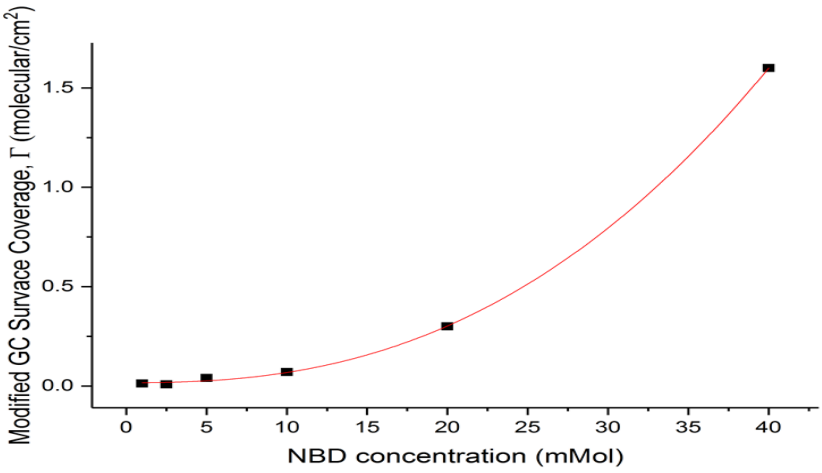

Figure 6.14 Oxidation correlation curve; between GC surface coverage of immobilised nitrobenzene diazonium tetrafluoroborate (NBD) modified anthraquinone, in pH 7 of KNO_3 and the concentration of nitrobenzene diazonium tetrafluoroborate (NBD).

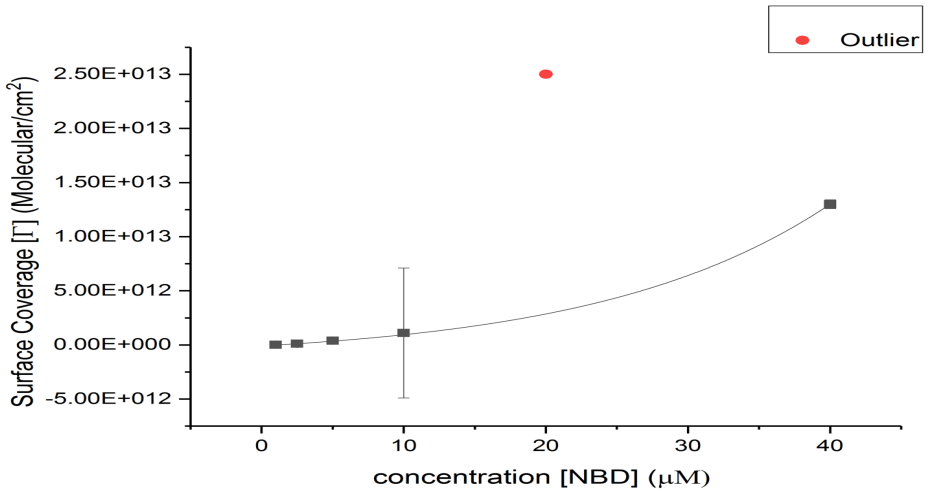

Figure 6.15 Reduction correlation curve; between GC surface coverage of immobilised nitrobenzene diazonium tetrafluoroborate (NBD) modified anthraquinone, in pH7 of KNO_3 and the concentration of nitrobenzene diazonium tetrafluoroborate (NBD). Where X and Y axis are the concentration of (NBD) and surface coverage.

The outlier: As result of interferance from peaks produced by the species reaching the anode (CE) from the solvent and interacting with AQ reduction peaks[41]. It is noticeable that increasing the rerponse in the reduction peak does not appear nor is it equivalent to the oxidation peak, this prove it is a result of irreversible reaction.[39] Hence, it can be as result of unstable components that are produce as a result of the oxygen activities such as $AQ^{\cdot-}$ or AQ $O_2^{\bullet--}$ or $O_2^{\bullet--}$. The ion $O_2^{\bullet--}$ ions are more likely to produce this high intensity of the reduction peak or H_2O_2.[33]

6.5. The Effect of the Multi-layers progression and the aryl Radicals.

The aryl radical, 4-aminonophenyl formation, mentioned in section (6.1), would cause branching growth progress[42] because they are bind to the benzene ring of oxidized ortho aryldiazonium on the monolayer surfaces, nonetheless they attack the aryl grafting groups. Consequently, these binding layers form multi layers which is crucial for the coupling reactions stage and causing multilayers formation.[43]

Therefore, basic rules are apply on the cyclic voltammetry when apply less current or voltage less diffusion of the redox active through the bulk or less deposition on GC electrodeieved.

Controling the multi or monolayer thickness could therefore be attained by adjusting the charge that consumed to produce the electro-grafted diazonium. The charge determination depends on the potential and the time applied in the potentsiostat. In practice applying to the cathode a potential equal to the voltammetry peaks (capacitance and faraday current) at the same time, reducing the charge that passing through the cell.[44] Additionally, the electrochemical signal measurment does not reflect the real NO_2 pheny groups that attach to the GC surface[45]

Interestingly, the reaction rate of the reduction of NO_2 was found to be limited by the charge transfer and not by the protons obtainability into the organic layer. A research was performed for the grafted NBD film reduction behaviour, combined with data collected by (FSG) spectroscopy.[46] Although, the potential was high enough to -1.0, with -0.1 more negative than this experiment, to convert all the NO_2 to NH_2, the closer NO_2 groups closer to the electrode surfaces would be reduced first to NH_2, followed by NHOH then another NO_2. In conclusion, the film produced exhibits a stratified structure. In addition, the peaks represents the NHOH and NH_2 were not quantitative as the SFG posed for long electrolysis time, this suggested that some of the nitro groups allocated far from the electrode surface. Successively, the electron tunnelling decline gradually away from the film thickness. At -0.8 V the NO_2 groups were reduced with the most quantitative generated NH_2. According to these findings, the occurrence of the stratified layer was explained by the unlimited H^+ cations diffusion in the organic film.[15]

Reducing the NBD on gold with the electro grafting process with 64% loss of the amount established by electroscopy, stretched by IRRAS and sonication in acetonitrile. This difference resembles un-grafted aryl cations that deposit physically and attached to the electrode surface.[47] These cations reduction occur by eliciting hydrogens from the solvent to produce dimerization according to the Gomberg Bachmann reaction law.[48] This problem can be resolved by rinsing the electrode with distilled water. Though, bonding of the organic layer is found to be very stable and can last for 6 months.[49] Therefore, more investigation about the stability of this layers and their interaction bond with GC surfaces need to be established for these modified concentrations.

Moreover, decreasing the aryl scavenger 2,2-diphenyl-1-picrylhydrazl concentration has found to cause decrease in the thickness, morphology and chemical composition of the grafted film. The radicals reduced before reaching the electrode. Consequently, the nitrophenyl would be grafted *via* the azo binding[50]. While the AFM and *X*-ray both established that the monolayer can be reach by radical trapping, not all nitrophenyl groups are electroactive in the film thicker than 2 nm[51]. Accordingly, other possible experiments can be established to study the effect of N, N-diisopropylethylamine (DIPEA or DIEA) concentration on the thickness of the layers under these experimental condition. Also, in this project the GC functionalised NBD-AQ carried out using the coupling agent EDC, as show in Figure 6.1. Although, the monolayer ranges has been achieved in these results.[52] In higher concentration which shows higher values for the surface coverages. Both possible layers of 4-nitrophenyl or 4-aminonopheyl progress rapidly on the GC electrode[53] which mostly occurs during the first step of grafted NBD[43], as shown in Figure 6.2. The solvent ACN causes the multilayers to swell and it has been explained as connected to the solvent and ions ingress and egress through association of the layer arrangement[54].

This study achieves the GC modification targets, eluding the complicated methodologies that aim to protect the NBD *para* position to reduce the multilayers formation. Such techniques are Boc-protected linker[51] or the mixture of BND and NBD, the strategies purposes are to create steric hindrance to prevent the aryl radical binding on the ortho-position of the NBD cyclic ring. Nevertheless, we found previously, that in *para* substitutions the reduction of the diazonium salts occurs within similar potential values.[55]

Furthermore, the multi-layer which are undesirable in DNA biosensors, are usually poorly conductor, hence, pose and cause barriers to electron transfer between electrode and the reduction species. In addition, the pausing of the signal of the distinguished reduction process after the first circle designates the inhibition of electron transfer to the NBD ions in solution, due to the formation of non-conducting grafted layer[56]. Subsequently, a slower electron transfer rate then blocks or deactivates the electrode. The structure of the reduced products has to be stable and of known density on the three dimensions structure in later stages for the probe and the DNA recognition stage[57].

7. Conclusion & Further Work

In this study, the electrochemical grafted NBD on GC surface electrode revealed successful surface coverage result when modified with redox active anthraquinone. Similarity, the GC surface NBD is controlled by the range of level optimum for the probe-target DNA detection, (1.6 – 6.6) $\times 10^{-12}$ molecules per cm^2 produced by 5, 2.5 mM of the diazonuim. However, the 1 mM NBD concentration also produced reliable result, the impurity need to be investigated by repeating the experiment with a fresh NBD samples or to increase the concentration by 0.2 mM to produce the appropriate signed grafted NBD voltammogram. The concentrations 10, 20 and 40 mM surface concentration results along with SC produced by 1, 2.5 and 5 mM produced very good oxidation and reduction correlations graphs with scan rate (SR), agree with the previous research in literature.

This experiment performed in this study offers a threshold of the NBD concentration that is required to produce electro-activities, under these condition,[58] saving time and cost by way of avoiding the use of blocking agents or BBD in previous studies. In addition, the precise concentration has to be optimised to produce adequate potential that do not destroy DNA.[59] The structure of multi or monolayers is measured by the grafted concentration of NBD at the GC surface Γ'_{sur} $\Gamma'_{volumme}$, the layer thickness, the density and model of the film and whether they contains pinholes.[60] However, it is challenging to deduce the structure of the compact layer and its behaviour in the aprotic solvent ACN during the electrochemical diffusion process[61]. For these reasons there is a need for other techniques to confirm these measurements. Therefore, these electrochemical surface coverages results and its calculations, need to be accompanied by AFM or the XPS for the analysis of the chemical composition to measure actual thickness or depth of the attached layer. Also, the correlation of AFM or PPF measurements with the surface density (Γ'/cm^{-2}) would provide the numbers of the mole binding to the surface.[62]

To this end, the basal plane electrode model has achieved successful modification. However, recently studies recognised a problem with the immobilisation on a bare surface of carbon as it tends to cause mutable interactions of transducer with phosphate backbone or hydrophobic nitrogenous bases of the investigated DNA or the snp's.[63] More research is required to test the effects of hydrogen bonds between the surface coverages and the solution to conform the agreement of the result with Density Functional Theory (DFT) and the functional modern available software.[64] Despite the fact that the electrodes modified diazonium salt increase electrode surface binding and stability, more explorative work is needed for those disposable fabricated electrode to enhance the commercial production scale in the point-of-care medicine and diagnostic fields.[39],[65]

The GC electron transfer can be determined according to Laviron theory and compared with the literature and edge plane. It is known that the edge plane presents faster electron transfer than the base plane electrode. The edge plane produces lower oxidation potential, higher oxidation current and narrower oxidation peak in contrast with the basal plane[66]. The basal plane of HOPG is found to produce less undesirable multilayers than the edge plane. Since the C graphene binding C ary[67]l converts from Sp^2 to Sp^3 bond, with less energy 24 kJ mol^{-1}. This is reasoning the edge plane has accessibility to form multilayers more than the base plane electrode since it tends to bind to the aryls radical diazonium to form Sp^3 bond rather than forming a compound using the Sp^2 bond. Added to this, if double layers of carbon binds in the para position they need higher value of energy of -264 kJ mol^{-1}, which is unfavourable covalent bond.[68] Also, this proved to supported with the AFM experiment findings.[69, 39]

In a recent publication, spatial heterogeneities within the same graphene working electrode occurred. This causing a greater reactivity at the edge and less reactivity if the surface electrode containing unexpected flake – flake area.[70] Thus, to produce accurate reliable outcome the integrity of surface of the electrode needed to be checked. A research project suggesting that the double graphene sheets and its chemical effects of Sp^2 would promote band gab and develop protocols through the concentration control and molecular design, which the modern method does not. Accordingly, improving graphene solubility and sensors functionality can be produced when the covalent grafted layers combined with nanostructured methods.[54,71]

In recent time, conventional nano-material electrode Au-nano self-assembled GCE biosensors proved to produced excellent selectivity for dsDNA and optimized probe-GCE when using CV techniques.[72] Also, the models CNT or SWCNT or screen-printed electrode (SPE) or carbon nano-onion (CNTo) of the nanotubes carbon material, have been found to become more popular in controlling surface coverage formation and selectivity.[73] Therefore, it possible to take advantages of those adequate GC or basal plane models of CNT as well as the edge Plane electrodes to examine the above variable concentration to gather more data for stabilities and multilayers formations. Also, to study the effects of the linkers NBD on the surface coverage and whether any overpowering effects of steric or electronic existence on the AQ coupling reaction. This can be accomplished by investigating the relationship between the binding energy and charge transfer.

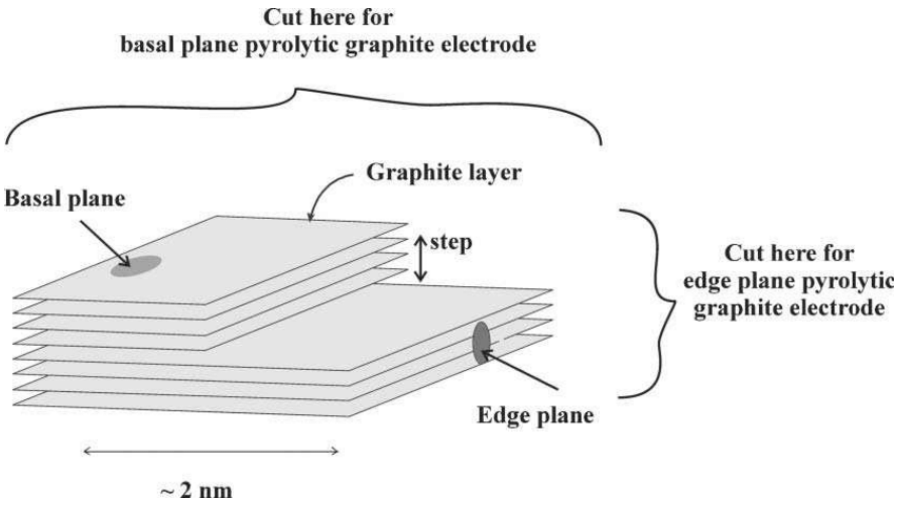

Figure 7 Illustration of the Basal Plane and Edge electrode or the HOPG (Highly Ordered Pyrolytic Graphite) adopted from Roy as Society of Chemistry[74]

8. References

1 W. Aktar, D. Sengupta and A. Chowdhury, *Interdiscip. Toxicol.*, 2009, **2**, 1–12.

2 S. Kumar, S. Tripathy, A. Jyoti and S. G. Singh, *Biosens. Bioelectron.*, 2019, 124–125, 205–215.

3 M. Zharnikov, in *Encyclopedia of Interfacial Chemistry: Surface Science and Electrochemistry*, Elsevier, 2018, pp. 375–380.

4 E. O. Blair and D. K. Corrigan, *Biosens. Bioelectron.*, 2019, 134, 57–67.

5 Biosensors: Fundamentals and Applications - Bansi Dhar Malhotra - Google Books, https://books.google.co.uk/books?id=LQBNDwAAQBAJ&pg=PA168&lpg=PA168&dq=6.A.A.+Khan+and+M.A.+Alzohairy,+Research+Journal+of+Biological+Sciences,+2010,+5,+565&source=bl&ots=K2SMdPt9KW&sig=ACfU3U1dEen7pmJj6Voo6k3-uj3Nj-YOIg&hl=en&sa=X&ved=2ahUKEwj9ntmM8NDoAhVjlFwKHToYBrQQ6AEwAXoECAsQKQ#v=onepage&q=6.A.A. Khan and M.A. Alzohairy%2C Research Journal of Biological Sciences%2C 2010%2C 5%2C 565&f=false, (accessed 5 April 2020).

6 V. Perumal and U. Hashim, *J. Appl. Biomed.*, 2014, 12, 1–15.

7 L. Angnes, E. M. Richter, M. A. Augelli and G. H. Kume, *Anal. Chem.*, 2000, **72**, 5503–5506.

8 A. M. Feltham and M. Spiro, *Chem. Rev.*, 1971, **71**, 177–193.

9 P. N. Bartlett, R. C. Alkire and J. Lipkowski, *Electrochemistry of carbon electrodes*, Wiley-VCH, 2015.

10 B. Meric, K. Kerman, D. Ozkan, P. Kara, S. Erensoy, U. S. Akarca, M. Mascini and M. Ozsoz, *Talanta*, 2002, **56**, 837–46.

11 N. Elgrishi, K. J. Rountree, B. D. McCarthy, E. S. Rountree, T. T. Eisenhart and J. L. Dempsey, *J. Chem. Educ.*, 2018, **95**, 197–206.

12 R. Y. Lai, B. Walker, K. Stormberg, A. J. Zaitouna and W. Yang, *Methods*, 2013, **64**, 267–275.

13 A. A. Rowe, K. N. Chuh, A. A. Lubin, E. A. Miller, B. Cook, D. Hollis and K. W. Plaxco, *Anal. Chem.*, 2011, **83**, 9462–9466.

14 Z. gang Yu, A. J. Zaitouna and R. Y. Lai, *Anal. Chim. Acta*, 2014, **812**, 176–183.

15 W. Richard, D. Evrard, B. Busson, C. Humbert, L. Dalstein, A. Tadjeddine and P.

Gros, *Electrochim. Acta*, 2018, **283**, 1640–1648.

16 G. Liu, J. Liu, T. Böcking, P. K. Eggers and J. J. Gooding, *Chem. Phys.*, 2005, **319**, 136–146.

17 C. Louault, M. D'Amours and D. Bélanger, *ChemPhysChem*, 2008, **9**, 1164–1170.

18 C. Esnault, N. Delorme, G. Louarn and J. F. Pilard, *ChemPhysChem*, 2013, **14**, 1793–1796.

19 P. A. Brooksby and A. J. Downard, *Langmuir*, 2005, **21**, 1672–1675.

20 O. Fontaine, J. Ghilane, P. Martin, J. C. Lacroix and H. Randriamahazaka, *Langmuir*, 2010, **26**, 18542–18549.

21 P. A. Brooksby and A. J. Downard, *J. Phys. Chem. B*, 2005, **109**, 8791–8798.

22 K. Malmos, J. Iruthayaraj, R. Ogaki, P. Kingshott, F. Besenbacher, S. U. Pedersen and K. Daasbjerg, *J. Phys. Chem. C*, 2011, **115**, 13343–13352.

23 T. Menanteau, E. Levillain and T. Breton, *Chem. Mater.*, 2013, **25**, 2905–2909.

24 J. M. Chrétien, M. A. Ghanem, P. N. Bartlett and J. D. Kilburn, *Chem. - A Eur. J.*, , DOI:10.1002/chem.200701559.

25 M. Velický, D. F. Bradley, A. J. Cooper, E. W. Hill, I. A. Kinloch, A. Mishchenko, K. S. Novoselov, H. V. Patten, P. S. Toth, A. T. Valota, S. D. Worrall and R. A. W. Dryfe, *ACS Nano*, 2014, **8**, 10089–10100.

26 J. Lehr, B. E. Williamson and A. J. Downard, *J. Phys. Chem. C*, 2011, **115**, 6629–6634.

27 M. Topsakal, H. Aahin and S. Ciraci, *Phys. Rev. B - Condens. Matter Mater. Phys.*, , DOI:10.1103/PhysRevB.85.155445.

28 M. Velický, D. F. Bradley, A. J. Cooper, E. W. Hill, I. A. Kinloch, A. Mishchenko, K. S. Novoselov, H. V. Patten, P. S. Toth, A. T. Valota, S. D. Worrall and R. A. W. Dryfe, *ACS Nano*, 2014, **8**, 10089–10100.

29 1d Philippe Allongue, 1b Michel Delamar, 1c Bernard Desbat, 1a Olivier Fagebaume, 1a Rachid Hitmi, *,1a and Jean Pinson and 1a Jean-Michel Savéant*, , DOI:10.1021/JA963354S.

30 M. Deschanels, F. Favier, O. Fontaine and S. Le Vot, *Electrochim. Acta*, 2020, **361**, 137027.

31 S. Daniele, M. A. Baldo, M. Corbetta and G. A. Mazzocchin, *J. Electroanal. Chem.*, 1994, **379**, 261–270.

32 Polymer Electrolyte Fuel Cells: Science, Applications, and Challenges - Google Books, https://books.google.co.uk/books?id=TN7MBQAAQBAJ&pg=PA149&lpg=PA149&dq=D.+J.+Schiffrin,+in+Electrochemistry,+ed.+D.+Pletcher,+The+Chemical+Society,+Burlington+House,+London,+1983,+vol.+8,+ch.+4.&source=bl&ots=idgwVPh1sl&sig=ACfU3U3TcdCNnW808nzae2GBv1vf9KuYZg&hl=en&sa=X&ved=2ahUKEwjm_oirxOnoAhViSxUIHd0YAFIQ6AEwAHoECAsQKQ#v=onepage&q=D. J. Schiffrin%2C in Electrochemistry%2C ed. D. Pletcher%2C The Chemical Society%2C Burlington House%2C London%2C 1983%2C vol. 8%2C ch. 4.&f=false, (accessed 15 April 2020).

33 D. Jeziorek, T. Ossowski, A. Liwo, D. Dyl, M. Nowacka and W. Woźnicki, *J. Chem. Soc. Perkin Trans. 2*, 1997, **0**, 229–236.

34 Electrochemical Reduction of Oxygen on Anthraquinone/Carbon Nanotubes Nanohybrid Modified Glassy Carbon Electrode in Neutral Medium, https://www.hindawi.com/journals/jchem/2013/756307/, (accessed 15 April 2020).

35 A. J. Downard, *Electroanalysis*, 2000, **12**, 1085–1096.

36 *J. Electroanal. Chem.*, 2003, **550**–**551**, iii.

37 C. E. Immoos, S. J. Lee and M. W. Grinstaff, *J. Am. Chem. Soc.*, 2004, **126**, 10814–10815.

38 Z. Zhu, … N. L.-J. D. to F. and P. and undefined 1998, *Wiley Online Libr.*

39 P. Yáñez-Sedeño, S. Campuzano and J. M. Pingarrón, *Sensors (Switzerland)*, 2018, 18.

40 M. T. McDermott, C. A. McCreery and R. L. McDermott, *Anal. Chem.*, 1993, **65**, 937–944.

41 A. J. Downard, *Electrochemically Assisted Covalent Modi®cation of Carbon Electrodes*, .

42 A. L. Gui, G. Liu, M. Chockalingam, G. Le Saux, E. Luais, J. B. Harper and J. J. Gooding, , DOI:10.1002/elan.201000164.

43 S. S. C. Yu, E. S. Q. Tan, R. T. Jane and A. J. Downard, *Langmuir*, 2007, **23**, 11074–11082.

44 J. Lipkowski, *J. Electroanal. Chem.*, 2003, 550–551, 1.

45 J. Pinson and F. Podvorica, *Chem. Soc. Rev.*, 2005, **34**, 429–439.

46 T. Menanteau, E. Levillain, A. J. Downard and T. Breton, *Phys. Chem. Chem. Phys.*, 2015, **17**, 13137–13142.

47 D. M. Shewchuk and M. T. McDermott, *Langmuir*, 2009, **25**, 4556–4563.

48 M. Gomberg and W. E. Bachmann, *J. Am. Chem. Soc.*, 1924, **46**, 2339–2343.

49 M. Delamar, G. Désarmot, O. Fagebaume, R. Hitmi, J. Pinson and J. M. Savéant, *Carbon N. Y.*, 1997, **35**, 801–807.

50 I. López, S. Dabos-Seignon and T. Breton, *Langmuir*, 2019, **35**, 11048–11055.

51 M. A. Ghanem, J. M. Chrétien, J. D. Kilburn and P. N. Bartlett, *Bioelectrochemistry*, 2009, **76**, 115–125.

52 J.-M. Chrétien, M. A. Ghanem, P. N. Bartlett and J. D. Kilburn, *Chem. - A Eur. J.*, 2009, **15**, 11928–11936.

53 A. L. Gui, G. Liu, M. Chockalingam, G. Le Saux, E. Luais, J. B. Harper and J. J. Gooding, *Electroanalysis*, 2010, **22**, 1824–1830.

54 S. Schauff, M. Ciorca, A. Laforgue and D. Bélanger, *Electroanalysis*, 2009, **21**, 1499–1504.

55 B. Barbier, J. Pinson, G. Desarmot, M. Sanchez, H. Hogeveen, G. F. Bickel, G. A. Olah, R. H. Schlosberg, Y. K. Mo and J. A. Olah, *Cyclic voltammetry in ACN + 0.1 M NBu4BF4 on a GC electrode (u Superacid-Catalyzed Protium-Deuterium Exchange in Isobutane Competing with tert-Butyl Cation Formation (5) (a*, Wiley, 1992, vol. 114.

56 L. Lee, H. Ma, P. A. Brooksby, S. A. Brown, Y. R. Leroux, P. Hapiot and A. J. Downard, *Langmuir*, 2014, **30**, 7104–7111.

57 P. H. Phong, D. T. Huyen, V. D. Loi, V. T. T. Ha, N. T. C. Ha, N. N. Ha and L. M. Thanh, *J. Nanoparticle Res.*, , DOI:10.1007/S11051-019-4573-7.

58 T. Menanteau, E. Levillain, A. J. Downard and T. Breton, *Phys. Chem. Chem. Phys.*, 2015, **17**, 13137–13142.

59 I. O. K'Owino, S. K. Mwilu and O. A. Sadik, *Anal. Biochem.*, 2007, **369**, 8–17.

60 A. J. Downard and M. J. Prince, *Langmuir*, 2001, **17**, 5581–5586.

61 M. Ceccato, L. T. Nielsen, J. Iruthayaraj, M. Hinge, S. U. Pedersen and K. Daasbjerg, *Langmuir*, 2010, **26**, 10812–10821.

62 Z. Abousalman-Rezvani, … P. E.-A. in C. and and undefined 2020, *Elsevier*.

63 B. Rafique, M. Iqbal, T. Mehmood and M. A. Shaheen, *Sens. Rev.*, 2019, 39, 34–50.

64 Associative and Proton Transfer Effects on the Voltammetric Behaviour of Chemically Grafted Films Bearing Nitrophenyl Groups - Ramírez-Delgado - 2020 - Electroanalysis - Wiley Online Library, https://onlinelibrary.wiley.com/doi/abs/10.1002/elan.201900367, (accessed 31 March 2020).

65 C. Jiang, S. Moraes Silva, S. Fan, Y. Wu, M. T. Alam, G. Liu and J. Justin Gooding, *J. Electroanal. Chem.*, 2017, **785**, 265–278.

66 W. Zhang, S. Zhu, R. Luque, S. Han, L. Hu and G. Xu, *Chem. Soc. Rev.*, 2016, 45, 715–752.

67 D. Bélanger and J. Pinson, *Chem. Soc. Rev.*, 2011, 40, 3995–4048.

68 M. Youssry, M. Al-Ruwaidhi, M. Zakeri and M. Zakeri, *Emergent Mater.*, 2020, **3**, 25–32.

69 J. K. Kariuki and M. T. McDermott, *Langmuir*, 1999, **15**, 6534–6540.

70 Y. Li, W. Li, M. Wojcik, B. Wang, L. C. Lin, M. B. Raschke and K. Xu, *J. Phys. Chem. Lett.*, 2019, **10**, 4788–4793.

71 F. M. Koehler, A. Jacobsen, K. Ensslin, C. Stampfer and W. J. Stark, *Small*, 2010, **6**, 1125–1130.

72 H. Z. Pan, H. W. Yu, N. Wang, Z. Zhang, G. C. Wan, H. Liu, X. Guan and D. Chang, *J. AOAC Int.*, 2015, **98**, 1728–1732.

73 J. Yang, K. Jiao and T. Yang, *Anal. Bioanal. Chem.*, 2007, **389**, 913–921.

74 C. E. Banks and R. G. Compton, *Analyst*, 2006, 131, 15–21.